Iterative Symbol Recovery for Power-Efficient DC-Biased Optical OFDM Systems

Amir Weiss, Arie Yeredor, *Senior Member, IEEE*, and Mark Shtaif, *Senior Member, IEEE, Fellow, OSA*

Abstract—Orthogonal frequency division multiplexing (OFDM) has proven itself as an effective multicarrier digital communication technique. In recent years, the interest in optical OFDM has grown significantly, due to its spectral efficiency and inherent resilience to frequency-selective channels and to narrowband interference. For these reasons, it is currently considered to be one of the leading candidates for deployment in short fiber links such as the ones intended for inter-data-center communications. In this paper, we present a new power-efficient symbol recovery scheme for dc-biased optical OFDM (DCO-OFDM) in an intensity-modulation direct-detection (IM/DD) system. We introduce an alternative method for clipping in order to maintain a nonnegative real-valued signal and still preserve information, which is lost when using clipping, and propose an iterative detection algorithm for this method. A reduction of 50% in the transmitted optical power along with an increase of signal-independent noise immunity (gaining 3 dB in SNR), compared to traditional DCO-OFDM with a dc bias of two standard deviations of the OFDM signal, is attained by our new scheme for a symbol error rate of 10^{-3} in a QPSK constellation additive white Gaussian noise flat channel model.

Index Terms—DC-biased optical orthogonal frequency division multiplexing, optical communication, power efficient.

I. INTRODUCTION

ALTHOUGH orthogonal frequency division multiplexing (OFDM) has been known for its advantages in quite a while [1]–[3], only in recent years it has turned into a major field of interest in optical communications [4], [5]. Particularly attractive is the intensity-modulation direct-detection (IM/DD) scheme, which, owing to its simple implementation and low cost, constitutes one of the leading candidates for inter-data-center communications. For such systems, the data is modulated onto an electrical signal, $x(t)$, which can be either voltage or current, depending on the details of the electrical system, and an optical intensity modulator generates an optical signal with intensity $\alpha x(t)$, where α is a real-valued positive coefficient. We emphasize that the light's intensity, and not its amplitude, is proportional to the electrical signal. Therefore, $x(t)$ must be a real-valued non-negative signal $x(t) \in \Re_+ \; \forall t$, which generally does not hold for an unconstrained baseband OFDM signal. In order to generate a real-valued baseband OFDM signal, the vector of symbols of length N (derived from a given constellation scheme), representing the bits, must meet the constraint

of Hermitian symmetry, thereby sacrificing half of the allocated bandwidth. After generating the real-valued signal, further modification is needed so as to meet the non-negativity condition. To this end, two primary methods have been proposed: asymmetrically clipped OFDM (ACO-OFDM) [6], [7] and dc-biased optical OFDM (DCO-OFDM) [8], [9]. ACO-OFDM is a method suggested by Armstrong and Lowery [6] where the OFDM signal is generated such that only the odd frequency subcarriers carry the information (i.e. symbols from a given constellation), and the even frequency subcarriers are set to zero. After the IFFT is applied, the signal is clipped at the zero level. In this form, all of the clipping noise falls on the even subcarriers, and the data carrying odd subcarriers remain undistorted. This method has been shown to be efficient in terms of optical power and from an information theoretic perspective [10], however it uses only one quarter of the available bandwidth, hence it is wasteful in terms of spectral efficiency. DCO-OFDM is a method in which a dc bias is added to the real-valued baseband OFDM signal in order to reduce the probability that it assumes negative values. Since, owing to the high peak to average power ratio (PAPR) characterizing OFDM, the positivity of the signal cannot be guaranteed with 100% certainty, the signal is clipped (i.e. its value is replaced by zero) in the intervals in which it is negative. The clipping operation causes distortion (mostly referred to as clipping noise) which limits the performance (in terms of symbol error rate (SER))[7]. The dc bias is set so as to ensure that the probability of a clipping event, and consequently the impact of clipping noise, remain acceptably low. The disadvantage of the DCO-OFDM is that the dc bias significantly increases the transmitted optical power. Several methods were proposed with the aim of addressing the power efficiency problem and coping with the implications of clipping noise. Most notable are the unipolar OFDM (U-OFDM) [11], which uses different time sample states and a rearrangement of the OFDM frame; asymmetrically companded DCO-OFDM (ADO-OFDM) [12], which uses a linear companding function in order to compress the negative part of the signal, thereby reducing the clipping noise, the Hartley Transform is proposed in [13] for optical IM/DD OFDM, and more. In this paper, we propose a new approach for meeting the non-negativity condition, which is based on replacing the negative parts of the dc-biased OFDM signal with their absolute value (AV). In this case the traditional clipping noise is replaced with a stronger noise contribution, but one that is correlated with the signal. By applying an iterative signs estimation algorithm (ISEA) which will be presented as well, our approach enables a significant reduction in the dc bias level, and a corresponding improvement in power efficiency. In Section II we review the mathematical model of an IM/DD channel and describe the

proposed alternative to the clipping method. In Section III we show simulation results where we compare the new suggested method to traditional DCO-OFDM and to a theoretical lower bound on performance. Section IV is devoted to conclusions.

II. A NEW APPROACH FOR MEETING THE NON-NEGATIVITY CONSTRAINT

We denote by $s(t)$ the data-carrying intensity waveform that is produced by the transmitter. After being photo-detected and electronically amplified, the electrical signal that impinges upon the analog to digital conversion unit (ADC) is given by

$$y(t) = s(t) + v(t), \tag{1}$$

where $v(t)$ is zero mean additive white Gaussian noise (AWGN) with variance σ_v^2. Equation (1) contains a simplified description of the optical channel, as it assumes that optical propagation effects, most prominently loss and chromatic dispersion, are compensated for prior to photo-detection. In addition, noise following from possible optical amplification is assumed to be negligible. It is assumed that the ADC resolution is sufficiently high in order to justify the neglect of quantization noise. Finally, Since a host of standard synchronization methods for optical OFDM communication systems is available [14], [15], we shall follow common practice by assuming perfect synchronization.

A. An Alternative to Clipping

Let $\{\alpha_i\}_{i=0}^{K-1}$ be a discrete, closed set of symbols from a given constellation (e.g., 16-QAM) denoted by $\mathcal{A}$, where K is the constellation size, and let $\{\theta_k\}_{k=0}^{N-1}$ be the series of symbols to be sent by the OFDM signal, where θ_k is the symbol corresponding to the k'th sub-carrier and N is the FFT size, such that $N = 2^m, m \in \mathbb{N}$. In order for the time-domain signal to be real-valued, the vector of symbols to be sent, $\boldsymbol{\theta}^T = [\theta_0 \ \theta_1 \ \ldots \ \theta_{N-1}]$, is constrained to Hermitian symmetry such that,

$$\theta_k = \theta_{N-k}^* , \ 0 < k < \frac{N}{2} \tag{2}$$

and the two components θ_0 and $\theta_{N/2}$ are set to zero, i.e. $\theta_0 = \theta_{N/2} = 0$. We assume $\{\theta_k\}_{k=0}^{N-1}$ are independent identically distributed random variables, distributed uniformly over the set $\mathcal{A}$, and $E[\theta_k] = 0$. Let $\{s[n]\}_{n=0}^{N-1}$ be the discrete-time signal at the IFFT output, corresponding to the vector of symbols $\boldsymbol{\theta}$, defined as

$$s[n] = \frac{1}{\sqrt{N}} \sum_{k=0}^{N-1} \theta_k e^{j\frac{2\pi}{N}kn} \tag{3}$$

$$= \frac{1}{\sqrt{N}} \sum_{k=1}^{N/2-1} \text{Re}\{\theta_k\} \cos\left(\frac{2\pi}{N}kn\right)$$

$$- \frac{1}{\sqrt{N}} \sum_{k=1}^{N/2-1} \text{Im}\{\theta_k\} \sin\left(\frac{2\pi}{N}kn\right) , \ 0 \le n \le N-1 \tag{4}$$

where the equality is due to (2), such that all $s[n]$ are real-valued. By the central limit theorem, if N is large enough, each sample $s[n]$ is approximately Gaussian distributed, with zero mean and variance σ_s^2 (derived from the constellation parameters). Once the digital OFDM signal is generated, the analog baseband OFDM signal is produced by a digital to analog converter (DAC). Assuming ideal reconstruction, by Shannon's interpolation formula we have

$$s(t) = \sum_{n=-\infty}^{\infty} s[n]p(t - nT_s) \tag{5}$$

where T_s denotes the sampling interval and $p(t) \triangleq \text{sinc}(t/T_s)$ is the ideal reconstruction kernel. Clearly, the condition $s(t) \in \Re$ is satisfied. At this point, in order to feed the electrical signal into the optical modulator, it is necessary to satisfy the non-negativity condition as well. In DCO-OFDM, a positive dc bias is introduced such that

$$s_B(t) \triangleq s(t) + B_{\text{DC}} , \ B_{\text{DC}} > 0 \tag{6}$$

where $s_B(t)$ is the biased baseband OFDM signal, and B_{DC} is the dc bias constant, commonly prescribed in terms of a proportionality constant κ, such that

$$B_{\text{DC}} \triangleq \kappa\sigma_s = \kappa\sqrt{E[s^2(t)]} , \ \kappa > 0 \tag{7}$$

is proportional to the standard deviation of $s(t)$. We define the bias-index as $\beta \triangleq 10\log_{10}(1 + \kappa^2)$[dB], where the log's argument is the ratio between the power of the biased signal $s_B(t)$ to the power of the original signal $s(t)$, which indicates the increase in power of $s_B(t)$ relative to $s(t)$. Since OFDM signals suffer from high PAPR, the biased signal still does not necessarily meet the non-negativity condition, which requires further manipulation of $s_B(t)$. A commonly used operation is clipping (at zero level), defined as

$$h(x) = \begin{cases} x, & x \ge 0 \\ 0, & x < 0. \end{cases}$$

Applied to the biased signal, the clipping operation yields the clipped signal

$$s_{c,B}(t) = \begin{cases} s_B(t), & s_B(t) \ge 0 \\ 0, & s_B(t) < 0 \end{cases} \tag{8}$$

and $s_{c,B}(t)$ is of course non-negative for all t, as required. However, this operation results in an additional noise component, usually referred to as clipping noise, since the clipped signal can be also described as

$$s_{c,B}(t) = s_B(t) + n_c(t) \tag{9}$$

where

$$n_c(t) \triangleq \begin{cases} 0, & s_B(t) \ge 0 \\ -s_B(t), & s_B(t) < 0 \end{cases} \tag{10}$$

is the clipping noise. The bias and the clipping noise are related to one another: on the one hand, increasing the bias is equivalent to reducing the clipping noise power, but the cost is of course higher transmitted optical power. On the other hand, reducing
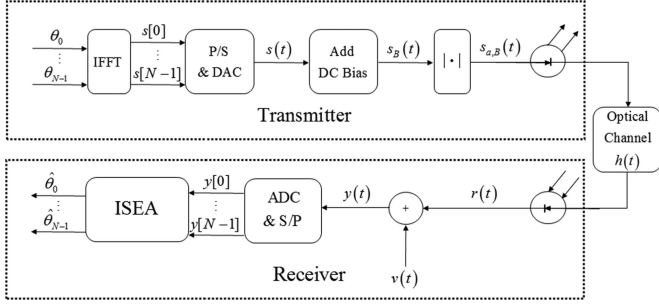
Fig. 1.   A block diagram of the transmitter and the receiver of the proposed modified DCO-OFDM.

the bias will save transmitted optical power, but at the same time will increase the clipping noise power, which may have an unacceptable effect on performance. The effect of clipping noise on performance can be seen in Armstrong and Schmidt's paper [7] for different bias and constellations. In practice, to achieve standard SER values for large constellations, a high signal to noise ratio (SNR) is required, so the clipping noise must be very low, therefore B_{DC} must be very large. Usually a bias of at least twice the standard deviation of the signal $s(t)$ must be used [16], [17], in order to reduce the clipping noise effect to tolerable levels (in terms of SER).

Clipping indeed ensures a non-negative signal, but at the expense of losing significant information. We propose to substitute the clipping operator with an AV operator

$$s_{a,B}(t) = |s_B(t)| . \tag{11}$$

The signal $s_{a,B}(t)$ still meets the non-negativity constraint, and at the same time it carries information that was lost by the clipping operation, and is not available in the clipped signal $s_{c,B}(t)$. Of course, this additional information is gained at the cost of losing the sign information of all values for all t. Nevertheless, as we demonstrate in what follows, the use of $s_{a,B}(t)$ turns out to be highly beneficial in the context of the OFDM detection process.

B. System Model

The block diagram of the proposed modified DCO-OFDM system is presented in Fig. 1. On the transmitter side, after applying the N-size IFFT to the constellation symbols so as to obtain the discrete-time signal, passing through the DAC and adding a dc bias, the AV operation replaces clipping. Similarly to most analyses of clipped OFDM systems [7], [12], [16], we do not include the effects of hardware induced bandwidth limitations, leaving this item for future study. After the AV is applied, the electrical (real-valued non-negative) baseband signal modulates the optical intensity of the laser output and the signal is sent through the optical channel. On the receiver side, the measured signal $y(t)$ is sampled by the ADC at the same rate that was used at the transmitter's DAC. Note that this sampling rate is not the Nyquist rate of $s_{a,B}(t)$, because of the bandwidth-expanding AV operation (similarly to the clipping operation), but this is immaterial since we are not interested in reconstructing

$s_{a,B}(t)$. As stated earlier in the beginning of this section, synchronization is assumed. Hence, we now have

$$y[n] = s_{a,B}[n] + v[n] , \ 0 \leq n \leq N - 1. \tag{12}$$

The samples $\{y[n]\}_{n=0}^{N-1}$ are sent as an input to the ISEA block for the symbols recovery process.

C. Iterative Signs Estimation Algorithm

We start by introducing the ISEA algorithm and its principle of operation while ignoring the presence of additive noise, i.e. with $\sigma_v^2 = 0$. The performance of the algorithm in the presence of additive noise will be considered numerically in Section III.

We will now show how the signs of the samples $\{s_B[n]\}_{n=0}^{N-1}$ are extracted (with high probability) from $\{y[n]\}_{n=0}^{N-1}$, which contains only their AVs. Let $\{z[n]\}_{n=0}^{N-1}$ be the (unknown) signs series, corresponding to the series $\{s_B[n]\}_{n=0}^{N-1}$, i.e.

$$z[n] \triangleq \text{sgn}\,(s_B[n]) = \begin{cases} +1, & s_B[n] \geq 0 \\ -1, & s_B[n] < 0 \end{cases} , \ 0 \leq n \leq N - 1 \tag{13}$$

where 0 is arbitrarily referred to as positive. The series of pairs $\{(y[n], z[n])\}_{n=0}^{N-1}$ contains complete information about $\{s_B[n]\}_{n=0}^{N-1}$ since $s_B[n] = z[n] \cdot y[n]$. In order to simplify the exposition, we define the following N-dimensional vectors

$$\mathbf{s} = [s[0] \ s[1] \ \ldots \ s[N-1]]^T, \mathbf{z} = [z[0] \ z[1] \ \ldots \ z[N-1]]^T$$

$$\mathbf{y} = [y[0] \ y[1] \ \ldots \ y[N-1]]^T, \boldsymbol{\theta} = [\theta_0 \ \theta_1 \ \ldots \ \theta_{N-1}]^T . \tag{14}$$

The ISEA strives to discover the true values of the series $\{z[n]\}_{n=0}^{N-1}$, and operates as follows:
1) (Initialization) set $i \leftarrow 0$ and $\hat{\mathbf{z}}^{(0)} = \mathbb{1}$.
2) Compute the estimated OFDM signal

$$\hat{s}^{(i)}[n] = \hat{z}^{(i)}[n] \cdot y[n] - B_{DC} , \ 0 \leq n \leq N - 1. \tag{15}$$

3) Compute the "soft" symbols estimators

$$\hat{\bar{\boldsymbol{\theta}}}^{(i)} = \text{FFT}\left\{\hat{\mathbf{s}}^{(i)}\right\}. \tag{16}$$

4) Compute the "hard" symbols estimators

$$\hat{\boldsymbol{\theta}}^{(i)} = \text{Slicer}\left\{\hat{\bar{\boldsymbol{\theta}}}^{(i)}\right\}. \tag{17}$$

5) If $\hat{\boldsymbol{\theta}}^{(i)} = \hat{\boldsymbol{\theta}}^{(i-1)}$ (and $i \neq 0$)
   a) return $\hat{\boldsymbol{\theta}}^{(i)}$.
6) Otherwise,
   a) $i \leftarrow i + 1$.
   b) Compute the updated estimated OFDM signal

$$\hat{\mathbf{s}}^{(i)} = \text{IFFT}\left\{\hat{\boldsymbol{\theta}}^{(i-1)}\right\}. \tag{18}$$

   c) Compute the updated sign estimators

$$\hat{\mathbf{z}}^{(i)} = \text{sgn}\left\{\hat{\mathbf{s}}^{(i)} + \mathbb{1} \cdot B_{DC}\right\}. \tag{19}$$

   d) Return to step (2).

Here, $\mathbb{1}$ denotes an $N \times 1$ all-ones vector, FFT$\{\cdot\}$ and IFFT$\{\cdot\}$ denote the FFT and IFFF operations, respectively,

Slicer$\{\cdot\}$ denotes the operation of assigning the valid symbol (from the given constellation) with the minimum Euclidian distance to its corresponding "soft" estimator, i.e.

$$\hat{\theta}_k = \underset{\theta \in \mathcal{A}}{\arg\min} \left\| \theta - \hat{\tilde{\theta}}_k \right\|^2, \qquad (20)$$

for each entry of $\hat{\boldsymbol{\theta}}$, sgn$\{\cdot\}$ denotes the sgn$(\cdot)$ operation elementwise, and $^{(i)}$ denotes the i'th iteration. Note that generally the "soft" estimator may be an invalid symbol, i.e. $\hat{\tilde{\theta}}_k \notin \mathcal{A}$.

Analysis of the algorithm in terms of theoretical runtime boundaries and probability of convergence (to the correct solution or at all) is cumbersome, as the complexity of the problem grows rapidly with the FFT size N. For example, an analytical assessment of the probability of an "Error Event" (upon convergence) defined as

$$\Pr(\epsilon) \triangleq \Pr\left(\hat{\boldsymbol{\theta}}^{(i)} = \hat{\boldsymbol{\theta}}^{(i-1)} \cap \hat{\boldsymbol{\theta}}^{(i)} \neq \boldsymbol{\theta} \right), \qquad (21)$$

is highly impractical. In order to do this, one must go over all the possible combinations and find all cases for which the "soft" estimators of two consecutive iterations, determined by two (possibly non-identical) sign series, result in the same "hard" estimator after the Slicer operation. However, the empirical determination of some useful parameters regarding the algorithm's performance, for a fixed set of system parameters (e.g., constellation type and size, signal power, dc bias etc.), is both simple and informative, and as we demonstrate numerically in Section III, the algorithm converges in only a few iterations to the correct solution for a moderate dc bias. Intuitively, the algorithm's logic can be explained in the following manner: the AVs information contained in the measurements reduces the problem to finding the correct signs. If a sufficient number of samples are assigned with their true original sign, the distortion caused by the AV operation, which will be referred to as AV noise (to be further discussed in what follows), will be tolerable (very much like the clipping effect), in the sense that the algorithm will have sufficient knowledge for correcting the wrongly guessed signs (in the initialization) by the discrete Fourier transform relation between the symbols and the OFDM signal and the prior information about the valid symbols, derived from the chosen constellation. Notice that in step (2), $\hat{\mathbf{s}}^{(i)}$ is updated by $\hat{\mathbf{z}}^{(i)}$, which is also updated in each iteration, and by the measurements $\mathbf{y}$, which remain unchanged. In this way, the set of signs being assigned to the measurements is updated iteratively, until the "best fit" is found, where "best fit" is defined by the stopping criterion—a series of signs for which the algorithm detects in the current iteration a vector of symbols identical to the detected vector of symbols in the preceding iteration. Obviously, if the initial signs series is the true signs series, the algorithm stops after two iterations, since no update will occur. The proposed algorithm is somewhat similar in its logic to the DAR algorithm, proposed by Kim and Stüber in [18], but its uniqueness clearly comes from handling the AV samples and updating the signs in each iteration by that information. In the next subsection we shall discuss the distortion caused by the AV operation, and shed light on the influence of the key parameters on the proposed method.

D. AV Noise

Much like the clipped signal, the AV signal can be written as the sum of the biased signal and a noise component, which will be called AV noise so that

$$s_{a,B}(t) = s_B(t) + n_a(t), \qquad (22)$$

where $n_a(t)$ denotes the AV noise, and is defined as

$$n_a(t) \triangleq \begin{cases} 0, & s_B(t) \geq 0 \\ -2s_B(t), & s_B(t) < 0. \end{cases} \qquad (23)$$

Note that the AV noise equals exactly two times the noise due to clipping. In a synchronized signal-independent-noiseless system, we have

$$y[n] = s_B[n] + n_a[n] \qquad (24)$$

where $n_a[n]$ are the samples of $n_a(t)$. Since by virtue of the central limit theorem, the sample $s[n]$ can be approximated as Gaussian distributed with zero mean and variance σ_s^2 (for each n), it follows that

$$s_B[n] \sim N(B_{\mathrm{DC}}, \sigma_s^2). \qquad (25)$$

Therefore,

$$\Pr(s_B[n] < 0) = Q\left(\frac{B_{\mathrm{DC}}}{\sigma_s} \right) = Q(\kappa) \triangleq p_a, \qquad (26)$$

where $Q(\cdot)$ denotes the standard Q-function, defined as

$$Q(x) = \frac{1}{\sqrt{2\pi}} \int_t^\infty \exp\left(\frac{-t^2}{2} \right) \mathrm{d}t, \qquad (27)$$

so the AV noise can be characterized by

$$n_a[n] = \begin{cases} 0, & w.p.\ 1 - p_a \\ -2s_B[n], & w.p.\ p_a. \end{cases} \qquad (28)$$

The mean and power of the AV noise can be analytically computed and are given (in terms of the proportionality constant κ) by

$$E[n_a[n]] = 2\sigma_s \left[\frac{1}{\sqrt{2\pi}} e^{\frac{-\kappa^2}{2}} - \kappa \cdot Q(\kappa) \right], \qquad (29)$$

$$E[n_a^2[n]] = 4\sigma_s^2 \left[(1 + \kappa^2)Q(\kappa) - \frac{\kappa}{\sqrt{2\pi}} e^{\frac{-\kappa^2}{2}} \right]. \qquad (30)$$

Fig. 2 shows simulation results that verify these analytical terms, for a true OFDM signal. By this representation, one can learn about the influence of the dc bias, the original OFDM signal's power and the ratio between them. Notice that when $B_{\mathrm{DC}} \gg \sigma_s$, namely $\kappa \gg 1$, the AV noise is highly unlikely to appear, so that $p_a \approx 0$. As we demonstrate in Section III, simulations of the proposed method in a broad range of system parameters reveal a threshold phenomenon—for a fixed set of system parameters the algorithm converges to the correct solution if the number of errors in the initial signs assignment does not exceed a certain threshold, typically much smaller than the FFT size, N. Otherwise, the AV noise effect becomes too dominant and the algorithm fails by converging to a false solution. We emphasize that the threshold number of errors depends on the constellation
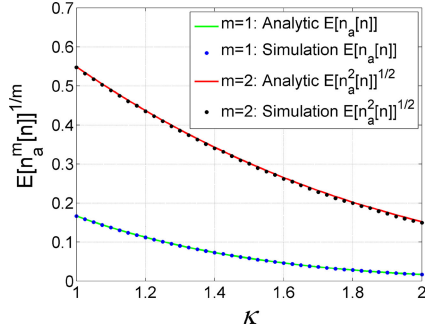
Fig. 2. Analytical and simulation results for the AV noise mean and root mean square (RMS) with $N = 1024$, $\sigma_s^2 = 1$ as the system parameters. Simulation results are based on averaging 2000 OFDM realizations, corresponding to a total of $\sim 10^6$ symbols.

type and size, and more precisely on the symbol density (i.e. the minimal Euclidian distance between two symbols), and the FFT size, N, because it affects the accuracy of the Gaussianity assumption, on which the procedure relies. In what follows, we denote by p_{th} the ratio between the threshold number of errors and the FFT size.

The statistical independence between the transmitted data symbols implies that the samples $s_B[n]$ are pairwise uncorrelated. In addition, by virtue of the central limit theorem, they are approximately Gaussian distributed for large N, and hence it is a reasonable approximation to treat them as if they were also statistically independent. In view of the above, our approach will be to choose the system parameters such that

$$p_a < p_{\mathrm{th}}, \qquad (31)$$

with the idea that this will lead to the convergence of the ISEA algorithm to the correct solution with high probability. Once p_{th} is known, an estimate of the smallest sufficient bias level can be obtained after substituting Eq. (26) in Eq. (31), yielding

$$B_{\mathrm{DC}} > \sigma_s \cdot Q^{-1}(p_{\mathrm{th}}). \qquad (32)$$

One can choose the OFDM signal power σ_s^2 based on the level of the additive noise (so as to guarantee adequate SNR) and then use Eq. (32) to find a bias level that would ensure convergence of the ISEA algorithm. These ideas are further investigated in the following section.

III. SIMULATION RESULTS

We shall present results for two systems with an FFT size of $N = 1024$, normalized signal power $\sigma_s^2 = 1$, and constellations of type QPSK and 8-PSK. First, we consider the case of a signal-independent-noiseless channel and examine clipping noise versus AV noise. Figs. 3 and 4 show the constellation diagrams of the traditional and the proposed DCO-OFDM methods for QPSK and 8-PSK respectively. As seen, a relatively low dc bias with $\kappa = 1$ and $\kappa = 1.3$ is applied for QPSK and 8-PSK respectively, and while the proposed method's estimators (before the slicer) are exactly the true values, the clipped signal suffers from a significant distortion, which makes it much more vulnerable to signal-independent noise. We remind that typical values for the dc bias used in traditional DCO-OFDM are at
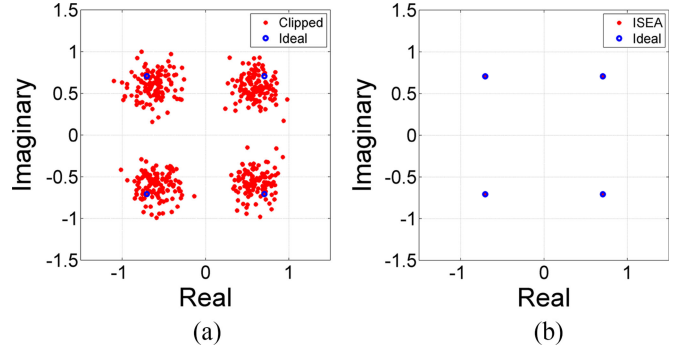

Fig. 3. Constellation diagram of QPSK. (a) Estimators before slicer for Traditional DCO-OFDM (via clipping) with $\beta = 3$ dB. (b) Estimators before slicer for the proposed method (via ISEA) with $\beta = 3$ dB.
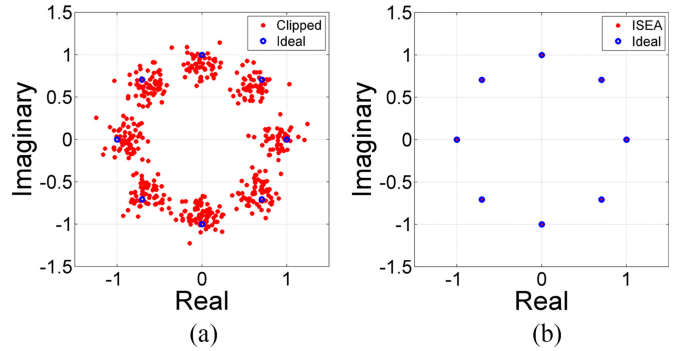

Fig. 4. Constellation diagram of 8-PSK. (a) Estimators before slicer for Traditional DCO-OFDM (via clipping) with $\beta = 4.3$ dB. (b) Estimators before slicer for the proposed method (via ISEA) with $\beta = 4.3$ dB.
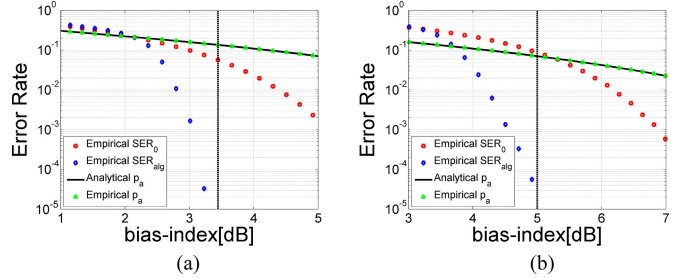

Fig. 5. Simulation results of initial SER (SER$_0$), ISEA's SER (SER$_{alg}$), analytical and empirical p_a with $N = 1024$, $\sigma_s^2 = 1$ and $\sigma_v^2 = 0$ based on averaging 4000 OFDM realizations, corresponding to a total of $\sim 10^6$ symbols. The horizontal axis is the bias-index defined as $\beta \triangleq 10 \log_{10}(1 + \kappa^2)$. The dashed line marks the bias level above which SER$_{alg} = 0$. (a) QPSK constellation (b) 8-PSK constellation.

least two standard deviations ($\kappa \geq 2$) of the OFDM signal, and Figs. 3 and 4 show the symbols estimators for QPSK with $\kappa = 1$ and for 8-PSK with $\kappa = 1.3$, only 50% and 65% respectively of the minimal conventional value (which reduces the transmitted optical power by 60% and 46% respectively). Clearly, the proposed method achieves satisfactory results with a significantly reduced dc bias. Fig. 5 shows the SER, defined as the number of incorrectly estimated symbols divided by the total number of symbols, as a function of the bias level with and without using the algorithm for QPSK and 8-PSK. The numerically assessed value of p_a is also shown in the figure, together with
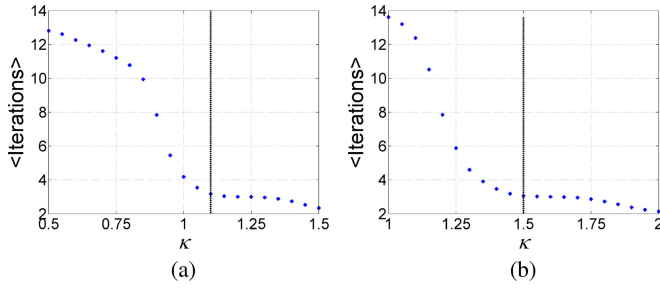
Fig. 6. The average number of iterations to convergence with $N = 1024$, $\sigma_s^2 = 1$ and $\sigma_v^2 = 0$ based on averaging 4000 OFDM realizations, corresponding to a total of $\sim 10^6$ symbols. The dashed line marks the bias level above which $SER_{alg} = 0$. (a) QPSK constellation. (b) 8-PSK constellation. The average number of iterations to convergence is 3.0024 with QPSK, and 3.0166 for 8-PSK, obtained with $\kappa = 1.2$ and $\kappa = 1.55$, respectively. The respective standard deviations were 0.06 and 0.13. In all 4000 realizations the maximum observed number of iterations to convergence was 4.

the analytical curve obtained from Eq. (26). The dotted vertical line indicates the bias level beyond which the ISEA algorithm converges to the exact value (SER= 0). The value of p_{th} corresponds to the intersection of this dotted vertical line with the curve describing p_a. Notice that the values of p_{th} are 0.1355 and 0.06654 in the cases of QPSK and 8-PSK, respectively. The corresponding respective values of B_{DC} in Fig. 5(a) and (b) are 1.1 and 1.5, and they can be checked to agree well with estimates based on Eq. (32). Fig. 6 shows the average number of iterations needed for the ISEA algorithm to converge as a function of the bias for QPSK and 8-PSK. Here too, the vertical dotted lines indicate the threshold bias level (as obtained from Fig. 5(a) and (b)). Evidently, when the algorithm converges to the correct solution (i.e. over the threshold), it does so within only few iterations.

We now move on to assessing the performance of the ISEA algorithm in the presence of AWGN (i.e. with $\sigma_v^2 > 0$). In this case we compare the ISEA performance not only with the that of the standard clipping method, but also with the performance of the selective mapping (SLM) method, which combats clipping noise by means of PAPR reduction [19], and was selected as a typical representative of the PAPR mitigation approach. The SLM method was implemented exactly as detailed in [19], using 128 alternative transmit sequences.[1] This number is significantly higher than the typical numbers used in SLM implementations, and hence the SLM results that we report can be viewed as an effective upper-bound for this method's performance. The comparison of the ISEA approach with the SLM method will be relevant when considering the complexity implications in what follows. In addition, we also show the results for an AWGN channel that is not subject to the non-negativity constraint (where $y[n] = s[n] + v[n]$), and hence its SER constitutes a theoretical lower bound.

We now examine the dependence of the SER on the SNR in the cases of QPSK and 8-PSK transmission, with the bias
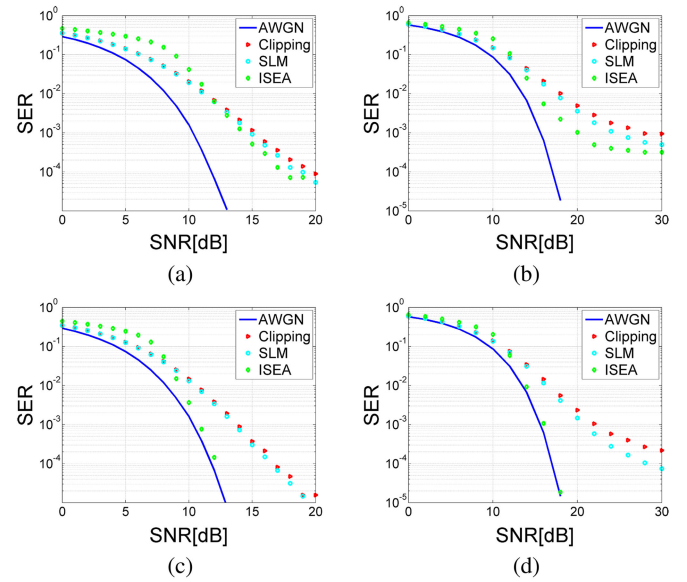

Fig. 7. Simulation results of SER versus SNR with $N = 1024$ and $\sigma_s^2 = 1$ based on averaging 2000 OFDM realizations, corresponding to a total of $\sim 10^6$ symbols. (a) QPSK constellation with $\beta = 3.35$ dB ($\kappa = 1.08$). (b) 8-PSK constellation with $\beta = 4.71$ dB ($\kappa = 1.4$). (c) QPSK constellation with $\beta = 3.87$ dB ($\kappa = 1.2$). (d) 8-PSK constellation with $\beta = 5.12$ dB ($\kappa = 1.5$).
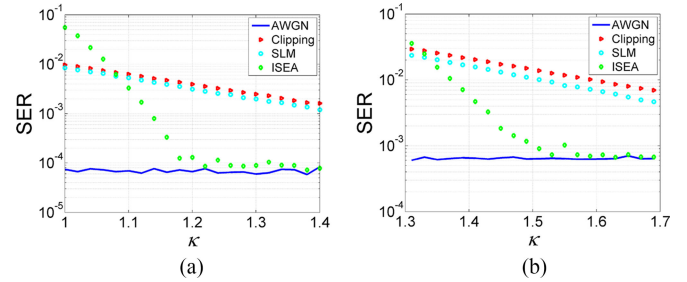

Fig. 8. Simulation results of SER versus κ for fixed SNR with $N = 1024$ and $\sigma_s^2 = 1$ based on averaging 2000 OFDM realizations, corresponding to a total of $\sim 10^6$ symbols. (a) QPSK constellation with SNR= 12 dB. (b) 8-PSK constellation with SNR= 16 dB.

levels set slightly below and slightly above the corresponding thresholds (recall that the threshold κ is 1.1 in the case of QPSK and 1.4 with 8-PSK, as seen in Fig. 6). Fig. 7(a) and (b) show the SER versus the SNR [defined as $10 \log_{10}(\sigma_s^2/\sigma_v^2)$] slightly below the κ-threshold, whereas in Fig. 7(c) and (d) κ is slightly higher than the threshold value. When κ is set slightly below the threshold [see Fig. 7(a) and (b)], the performance of the ISEA and the two other clipping-based methods are comparable in the low SNR regime, but in the relevant range, with the SER set to 10^{-3} the ISEA scheme gains relative to the other methods. With QPSK the ISEA result is similar to that of SLM and it is ~ 1 dB better in SNR than in the case of standard clipping. With 8-PSK the SNR gain with respect to standard clipping and SLM, is 8 and 4 dB, respectively. When κ is slightly above the threshold value [see Fig. 7(c) and (d)], the performance of the ISEA method rapidly converges to the performance of the unconstrained AWGN channel, implying that the positivity requirement does not introduce any penalty. Figure 8 shows the

[1]Each transmit sequence is generated via an element by element multiplication by a phase vector, whose N elements are constrained to Hermitian symmetry, so that $N/2 - 1$ of them are chosen randomly (and uniformly) from the set $\{-1, +1\}$. Furthermore, we assume that the phase vector of the chosen lowest PAPR sequence is known to the receiver.

TABLE I

Constellation	κ	SNR Gain [dB]
QPSK	1.2	3
8-PSK	1.5	6.1
16-PSK	2.1	4.2
16-QAM	2.1	1.47

Threshold Values of κ and the SNR Gain, With Respect to the Standard DCO-OFDM Method, for a Fixed SER of 10^{-3}, With $N = 1024$ and $\sigma_s^2 = 1$. In all cases the ISEA method outperforms clipping.
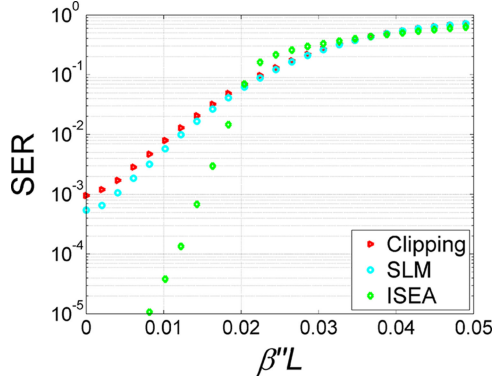

Fig. 9. Simulation results of SER versus the normalized dispersion $B^2 \beta'' L$ where B is the channel bandwidth, β'' is the dispersion coefficient, and L is the length of the link. The curves were obtained with $N = 1024$, $\sigma_s^2 = 1$, $\kappa = 1.6$ and SNR= 20 dB in 8-PSK constellation. Results are based on averaging 2000 OFDM realizations, corresponding to a total of $\sim 10^6$ symbols.

SER versus κ for a fixed SNR value, illustrating the difference between the various methods below and above the threshold value of κ. Note that unlike in the case of the other two methods, the performance of the ISEA scheme rapidly approaches the theoretical lower bound. Table I shows the threshold values of κ and the gain in SNR with respect to standard bias and clipping with the SER set to 10^{-3} for a few common constellations. As seen, the proposed method outperforms clipping in SNR requirement while reducing the dc bias. It is noteworthy that the dc bias threshold was computed for a noiseless channel, hence the threshold in a noisy channel would most likely be higher for low SNRs and would approach the noiseless threshold as the SNR increases. This explains the degraded performance of the proposed method for low SNRs, expressed by the gap between the lower bound and ISEA's curves in the low SNR region of Fig. 7(c) and (d).

In Fig. 9 we compare the tolerance of the three methods to chromatic dispersion. It should be noted in this context that schemes based on direct laser modulation, such as the ones that we are considering, are not intended for highly dispersive links. Yet, comparing the three schemes with respect to this phenomenon can be viewed as a plausible indicator of their relative tolerance to inter-symbol-interference mechanisms in a more general sense. Since the AV operation underpinning the ISEA approach produces larger spectral broadening than standard-clipping or SLM, the ISEA method is expected to be
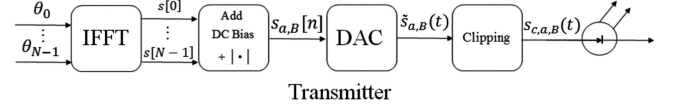

Fig. 10. A block diagram of the simplified transmitter, where dc bias addition and the AV operator are applied on the digital signal, such that $s_{a,B}[n] = |s[n] + B_{DC}|$.

less tolerant to dispersion. Indeed, this reality is seen in Fig. 9, where the rate at which the ISEA performance deteriorates with increasing dispersion is higher than it is with the other two approaches. Nonetheless, the vast advantage of the ISEA approach more than compensates for this sensitivity.

Finally, we wish to address the implications of the proposed ISEA method with respect to the complexity of the overall system. The receiver of the ISEA scheme involves one FFT and one IFFT operation per iteration and hence the complexity increase in comparison with the standard clipping-based DCO-OFDM approach, is determined by the number of iterations that are required for the algorithm to converge. As witnessed by the simulation results displayed in Fig. 6, the average of the number of iterations needed for convergence (above threshold) is practically equal to 3 and its standard deviation is between one order of magnitude and two orders of magnitude smaller.[2] This implies that the effective complexity of the ISEA method is larger by a factor of 6 relative to standard clipping, where the receiver performs a single FFT operation. It is interesting to compare this cost, with the cost of a typical PAPR reduction method, such as SLM [19]. The SLM method also involves additional IFFT operations, whose number equals the number of alternative transmit sequences that it includes. Hence, an SLM method with the same complexity overhead as the ISEA would include 6 alternative transmit sequences, and its performance would be inferior to that of the SLM results that we have shown in Figs. 7–9, where the number of alternative transmit sequences was 128. Although we have only considered SLM explicitly, it must be noted that SLM is not considerably different from other PAPR reduction methods in terms of its complexity performance tradeoff.[3] All these methods aim at reducing the PAPR, as opposed to the ISEA method which *copes* with it. In this sense, the PAPR reduction methods are complimentary to the ISEA approach and in principle the two can be combined with one another.

We note in passing, that assuming synchronization, a scheme with the same receiver but with a different, significantly easier to implement transmitter will yield exactly the same results presented above. The simplified transmitter, proposed in Fig. 10, differs from the original by applying the dc bias and the AV operation digitally on the samples, followed by simple clipping after the DAC, to ensure non-negativity. In this manner, all the values at the samples instances are identical to those produced by the transmitter presented in Fig. 1, hence leading to identical results.

---

[2]This was also confirmed in simulations with a broad variety of system set-ups.

[3]Other relevant methods in this context are; partial transmit sequence, interleaving, tone reservation, and tone injection. As detailed in [19], [20] these methods also involve additional FFT/IFFT operations and/or solvers of optimization problems.

IV. CONCLUSION

We proposed a new approach for meeting the non-negativity constraint in IM/DD. The new scheme, combines the AV operator and the ISEA algorithm, and shows a significant improvement over the standard DCO-OFDM method, both in terms of SER performance for a given dc bias and in terms of the bias needed for a given required SER. With a relatively moderate dc bias-index of 3.87 and 5.12 dB for QPSK and 8-PSK respectively, the theoretical lower bound of a standard AWGN channel is achieved. Along with a rudimentary analysis of the AV noise, both analytically approximated lower bound on the dc bias and simulation results of the proposed method have been presented. Our analysis was performed for the case of a linear system, neglecting component imperfections and hence provides an upper bound for the system performance. The consideration of the tolerance of the scheme for system non-idealities is left for future study.

REFERENCES

[1] R. W. Chang, "Orthogonal frequency multiplex data transmission system," U.S. Patent 3 488 445, Jan. 6, 1970.
[2] J. Salz and S. Weinstein, "Fourier transform communication system," in *Proc. 1st ACM Symp. Problems Optim. Data Commun. Syst.*, 1969, pp. 99–128.
[3] A. Peled and A. Ruiz, "Frequency domain data transmission using reduced computational complexity algorithms," in *Proc. IEEE Int. Conf. Acoust., Speech, Signal Process.*, 1980, vol. 5, pp. 964–967.
[4] B. J. Dixon, R. D. Pollard, and S. Iezekiel, "Orthogonal frequency-division multiplexing in wireless communication systems with multimode fiber feeds," *IEEE Trans. Microw. Theory Tech.*, vol. 49, no. 8, pp. 1404–1409, Aug. 2001.
[5] J. Armstrong, "OFDM for optical communications," *J. Lightw. Tech.*, vol. 27, no. 3, pp. 189–204, Feb. 2009.
[6] J. Armstrong and A. Lowery, "Power efficient optical OFDM," *Electron. Lett.*, vol. 42, no. 6, pp. 370–372, 2006.
[7] J. Armstrong and B. Schmidt, "Comparison of asymmetrically clipped optical OFDM and dc-biased optical OFDM in AWGN," *IEEE Commun. Lett.*, vol. 12, no. 5, pp. 343–345, May 2008.
[8] J. B. Carruthers and J. M. Kahn, "Multiple-subcarrier modulation for nondirected wireless infrared communication," *IEEE J. Sel. Areas Commun.*, vol. 14, no. 3, pp. 538–546, Apr. 1996.
[9] O. Gonzalez, R. Perez-Jimenez, S. Rodriguez, J. Rabadán, and A. Ayala, "OFDM over indoor wireless optical channel," *IEE Proc., Optoelectronics*, vol. 152, no. 4, pp. 199–204, 2005.
[10] X. Li, R. Mardling, and J. Armstrong, "Channel capacity of IM/DD optical communication systems and of ACO-OFDM," in *Proc. IEEE Int. Conf. Commun.*, 2007, pp. 2128–2133.
[11] D. Tsonev, S. Sinanovic, and H. Haas, "Novel unipolar orthogonal frequency division multiplexing (u-OFDM) for optical wireless," in *Proc. IEEE 75th Veh. Technol. Conf.*, 2012, pp. 1–5.
[12] F. Barrami, Y. Le Guennec, E. Novakov, and P. Busson, "An optical power efficient asymmetrically companded DCO-OFDM for IM/DD systems," in *Proc. 23rd IEEE Wireless Opt. Commun. Conf.*, 2014, pp. 1–6.
[13] M. Svaluto Moreolo, R. Muñoz, and G. Junyent, "Novel power efficient optical OFDM based on Hartley transform for intensity-modulated direct-detection systems," *J. Lightw. Technol.*, vol. 28, no. 5, pp. 798–805, Mar. 2010.
[14] H. Tang, K. Y. Lau, and R. W. Brodersen, "Synchronization schemes for packet OFDM system," in *Proc. IEEE Int. Conf. Commun.*, 2003, vol. 5, pp. 3346–3350.
[15] X. Jin and J. Tang, "Optical OFDM synchronization with symbol timing offset and sampling clock offset compensation in real-time IMDD systems," *IEEE Photon. J.*, vol. 3, no. 2, pp. 187–196, Apr. 2011.
[16] J. Armstrong, B. Schmidt, D. Kalra, H. A. Suraweera, and A. J. Lowery, "SPC07-4: Performance of asymmetrically clipped optical OFDM in AWGN for an intensity modulated direct detection system," in *Proc. IEEE Global Telecommun. Conf.*, 2006, pp. 1–5.
[17] M. Svaluto Moreolo, "Power efficient and cost-effective solutions for optical OFDM systems using direct detection," in *Proc. 12th Int. Conf. Transp. Opt. Netw.*, 2010, pp. 1–4.
[18] D. Kim and G. L. Stuber, "Clipping noise mitigation for OFDM by decision-aided reconstruction," *IEEE Commun. Lett.*, vol. 3, no. 1, pp. 4–6, Jan. 1999.
[19] L. Nadal, M. S. Moreolo, J. M. Fabrega, and G. Junyent, "Comparison of peak power reduction techniques in optical OFDM systems based on FFT and FHT," in *Proc. 13th Int. Conf. Transp. Opt. Netw.*, 2011, pp. 1–4.
[20] T. Jiang and Y. Wu, "An overview: Peak-to-average power ratio reduction techniques for OFDM signals," *IEEE Trans. Broadcast.*, vol. 54, no. 2, pp. 257–268, Jun. 2008.

Amir Weiss received the B.Sc. (*cum laude*) and M.Sc. degrees in electrical engineering from Tel-Aviv University, Tel-Aviv, Israel, in 2013 and 2015, respectively, where he is currently working toward the Ph.D. degree under the supervision of Prof. A. Yeredor with the School of Electrical Engineering, Department of Electrical Engineering Systems. His research and teaching areas are in statistical and digital signal processing and estimation theory. He has also been holding a researcher position in these research areas with Elbit Systems, EW and SIGINT Elisra Ltd., Bene Beraq, Israel, since 2013.

Arie Yeredor (M'99–SM'02) received the B.Sc. (*summa cum laude*) and Ph.D. degrees in electrical engineering from Tel-Aviv University (TAU), Tel-Aviv, Israel, in 1984 and 1997, respectively. He is currently an Associate Professor with the School of Electrical Engineering, Department of Electrical Engineering Systems, TAU, where his research and teaching areas are in statistical and digital signal processing and estimation theory. He also held a consulting position in these research areas with NICE Systems, Inc., Ra'anana, Israel, from 1990 to 2015. In 2015–2016, he has been on Sabbatical Leave from TAU as a Visiting Professor at the Georgia Institute of Technology, Atlanta, GA, USA. He previously served as an Associate Editor for the IEEE SIGNAL PROCESSING LETTERS, IEEE TRANSACTIONS ON CIRCUITS AND SYSTEMS—PART II: EXPRESS BRIEFS, and IEEE TRANSACTIONS ON SIGNAL PROCESSING, and also served as a Guest Editor for IEEE SIGNAL PROCESSING MAGAZINE's Special Issue on Source Separation and Applications. He served as a Technical Co-Chair of the 3rd International Workshop on Computational Advances in Multi-Sensor Adaptive Processing, as a General Co-Chair of the 10th International Conference on Latent Variables Analysis and Signal Separation (LVA/ICA2012), and as a Technical Co-Chair of LVA/ICA2015. He has been awarded the yearly Best Lecturer of the Faculty of Engineering Award (at TAU) seven times. He serves as a Member of the IEEE Signal Processing Society's Signal Processing Theory and Methods Technical Committee, and also serves as the Chair of the Signal Processing chapter of IEEE Israel Section.

Mark Shtaif (SM'99) received the M.Sc. and Ph.D. degrees in electrical engineering from the Technion—Israel Institute of Technology, Haifa, Israel, in 1993 and 1997, respectively. In 1997, he joined the Light-wave Networks Research Department at AT&T Labs Research as a Senior and then Principal Member of Technical Staff. At AT&T, his work centered on modeling and characterization of optical fiber communication systems focusing on propagation effects in optical fibers including fiber nonlinearities, polarization mode dispersion, special modulation formats, and interaction of signals and noise. During his employment, he consulted to the AT&T business units on the integration of fiber-optic technologies. In 2000, he became a Principal Architect in CelionNetworks, an optical networking company, where he worked on the analysis and design of long-haul optical transmission systems. In April 2002, he joined the School of Electrical Engineering, Tel-Aviv University, Tel-Aviv, Israel, where he is teaching and conducting research in areas related to fiber optics and optical communications. He is a Fellow of the Optical Society of America.